First Principles Calculations of the Tautomers and pK_a Values of 8-Oxoguanine: Implications for Mutagenicity and Repair

Yun Hee Jang,[†,‡] William A. Goddard III,*[,†] Katherine T. Noyes,[§] Lawrence C. Sowers,[†,§] Sungu Hwang,[‡] and Doo Soo Chung*[,‡]

Materials and Process Simulation Center, Beckman Institute (139-74), California Institute of Technology, Pasadena, California 91125, School of Chemistry, Seoul National University, Seoul 151-747, Korea, and Department of Biochemistry and Microbiology, Loma Linda University School of Medicine, Loma Linda, CA 92350

Received September 6, 2001

8-Oxoguanine is a mutagenic oxidative damage product of guanine that has been the subject of many experimental studies. Despite numerous references to this damaged base, its precise configuration or population of configurations in equilibrium are unknown, as it can be drawn in over 100 potential neutral and ionized tautomeric forms. The structural uncertainty surrounding 8-oxoguanine complicates mechanistic studies of its mutagenicity and capacity to be recognized for repair. Experimental measurements on the tautomeric equilibria and pK_a values of 8-oxoguanine are complicated by its insolubility in water. Therefore, we used first principles quantum mechanics (density functional theory, B3LYP, in combination with the Poisson−Boltzmann continuum-solvation model) to investigate the relative stabilities and site-specific pK_a values of various neutral and ionized tautomers of 8-oxoguanine. We show that the major tautomer of neutral 8-oxoguanine in aqueous solution is the 6,8-diketo form **2**, and that 8-oxoguanine has increased acidity at N1 relative to guanine. Our calculations on 2′-deoxyguanosine-3′,5′-bisphosphate and its 8-oxo analogue support the accepted conclusion that repulsion between the O8 of 8-oxoguanine and O5′ of the backbone sugar promote 8-oxoguanine:adenine pairings in the syn:anti conformation. Further, we show that the N7 proton of 8-oxoguanine is difficult to remove either through tautomerization or ionization, consistent with its involvement as an important landmark in distinguishing guanine from 8-oxoguanine. The possibility of additional structural landmarks that distinguish 8-oxoguanine from guanine, and a possible mechanism for glycosylase removal of 8-oxoguanine are discussed.

1. Introduction

The DNA of all living organisms is constantly damaged by reactive oxygen species (ROS). Among the many DNA oxidation damage products identified to date, substantial work has focused on 8-oxoguanine (8oxoG) (*1*−*3*), which is derived from the oxidation of guanine (Scheme 1). This damaged base is known to induce G:C to T:A transversion mutations (*4*−*7*), which can result from 8oxoG:A mispairing in the syn:anti conformation (*8*−*11*). When 8oxoG is paired with cytosine (*12*, *13*), it is repaired in humans by a specific glycosylase (hOgg1) that can distinguish 8-oxoguanine from guanine with high fidelity (*14*). The mechanisms by which the repair glycosylase can exploit the structural features of 8-oxoguanine to enhance discrimination for the damaged base and to facilitate glycosidic bond cleavage are not well understood. The specific placement of hydrogen bonding protons as well as their acid-base properties could play a significant role in allowing for discrimination between aberrant and normal bases by the repair glycosylase, as well as catalysis of glycosidic bond cleavage.

Scheme 1. 8-Oxoguanine

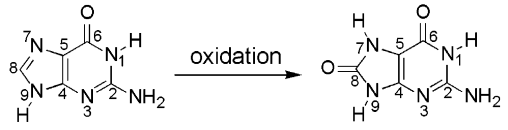

1 (guanine) **2** (8-oxoguanine)

A multitude of potential tautomeric forms can be drawn for 8-oxoguanine. In addition, many sites on 8-oxoguanine can be involved in either protonation or ionization. There are a total of 128 potential tautomeric and ionized forms that can be drawn for this oxidized base. It is as yet unknown if several tautomeric configurations of 8-oxoguanine could be of similar enough energy in various environments that they must be considered when exploring the potential biological consequences of this damaged DNA base. Limited experimental data are available on 8-oxoguanine derivatives. This limitation is in part because of the low water solubility of guanine and even more so that of 8-oxoguanine, as addition of oxygen atoms to purine derivatives often renders the more oxygenated species more insoluble than the original purine. As oxygen atoms are added in the series purine,

* To whom correspondence should be addressed. E-mail: (W.A.G.) wag@wag.caltech.edu and (D.S.C.) dschung@snu.ac.kr.
† Materials and Process Simulation Center.
‡ School of Chemistry, Seoul National University.
§ Department of Biochemistry and Microbiology, Loma Linda University School of Medicine.

10.1021/tx010146r CCC: $22.00
Published on Web 08/01/2002

hypoxanthine, xanthine and uric acid, the water solubility decreases by a factor of more than 10^4 (*15*).

Recently, we used first principles quantum mechanics (QM; density functional theory with generalized gradient approximation, B3LYP, in combination with the Poisson−Boltzmann (PB) continuum-solvation model) to predict pK_a values and proton configurations for a number of oxidized pyrimidines, which gave us results that closely correlate with experimental data (*16*, *17*). Given the experimental inaccessibility of much information regarding the structural preference (or preferences) of 8-oxoguanine, we have conducted a similar computational study of the possible proton configurations of this compound. To fully understand the biological consequences of this oxidized base, including its mutagenicity and capacity to be faithfully repaired, it is essential that we understand the precise structure, or population of structures, that make up the physiological existence of 8oxoG.

Our studies show, in accordance with others (*18*−*23*), that the predominant tautomeric form of 8-oxoguanine in water is the 6,8-diketo-2-amino tautomer, **2**, shown in Scheme 1. The N7 proton, the key structural element distinguishing 8-oxoguanine and guanine, is unlikely to move either due to tautomerization or ionization, perhaps providing a structural landmark that facilitates repair. The N1 proton is the most acidic of all the protons, perhaps decreasing the stability of the 8oxoG:C base pair. The most easily protonated site is N3, which may be involved in glycosylase-catalyzed base removal. The N9 proton of 8-oxoguanine is more acidic than the corresponding proton of guanine, also facilitating repair. The tendency of 8oxoG residues to flip into the normally nonpreferred syn conformation required for mispair formation is shown to result from a reduction in the repulsion between the 8-oxo oxygen of 8oxoG and oxygen atoms on the phosphate and sugar. The computational results that we present on the free base 8-oxoguanine are shown to correlate well with the experimental data that is available for the nucleoside and deoxynucleoside analogues 8-oxoguanosine and 8-oxodeoxyguanosine, respectively (*20*). This correlation supports the value of such computational methods when experimental data is either unavailable or inaccessible.

2. Calculation Details

The pK_a calculation was complicated due to the presence of multiple tautomers having differing pK_a values (site-specific or microscopic pK_as). A way to estimate the overall pK_a from the site-specific pK_as of the tautomers has been devised in a previous study that is currently under review. This study, wherein we use the same approach, is entitled "First Principles Calculations on the pK_a Values of Guanine in Water", and bears the same authors as the work presented here. All subsequent references to this work will be designated (Jang et al., unpublished results). We present sufficient details here to repeat the calculations.

2.1. Calculation of pK_a in the Presence of Multiple Tautomers. In the aqueous phase, tautomerization by the solvent-mediated proton transfer is expected to be fast compared to the time scale of the pK_a measurement, leading to the establishment of a rapid equilibrium between tautomers during the measurement. Assuming this rapid equilibrium, we calculate the pK_a values in the presence of multiple tautomers as follows.

Scheme 2. Simple Model Case for Illustrating the Calculation of pK_a in the Presence of Multiple Tautomers

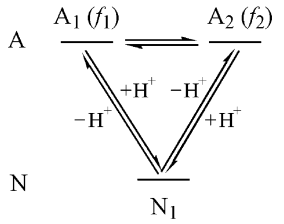

First we consider the simplest case, with only one tautomer at the protonated state (N) and two tautomers at the deprotonated state (A_1 and A_2; $[A] = [A_1] + [A_2]$) (Scheme 2). The free energy of deprotonation from N to A_1 and to A_2 is given by ΔG_1 and ΔG_2, respectively. The relative populations of the deprotonated tautomers, f_1 and f_2, are given by

$$f_1 = \frac{[A_1]}{[A]} = \frac{[A_1]}{[A_1] + [A_2]} \tag{1a}$$

$$f_2 = \frac{[A_2]}{[A]} = \frac{[A_2]}{[A_1] + [A_2]} \tag{1b}$$

where $f_1 + f_2 = 1$, $0 \le f_1 \le 1$, and $0 \le f_2 \le 1$. These populations are calculated from the Boltzmann distribution based on the relative free energies of those tautomers as done in the sections 3.1 to 3.3. The overall dissociation constant, K_a, is given as

$$K_a = \frac{[H^+][A]}{[N]} \tag{2}$$

The site-specific dissociation constants, K_a^1 and K_a^2, can be calculated from the free energies of deprotonation of the corresponding processes:

$$K_a^1 = \frac{[H^+][A_1]}{[N]} = \exp\left(-\frac{\Delta G_1}{RT}\right) \tag{3a}$$

$$K_a^2 = \frac{[H^+][A_2]}{[N]} = \exp\left(-\frac{\Delta G_2}{RT}\right) \tag{3b}$$

Equations 1−3 can be rewritten as

$$K_a^1 = \frac{[H^+][A_1]}{[N]} = \frac{[H^+][A]}{[N]} f_1 = K_a f_1 \tag{4a}$$

$$K_a^2 = \frac{[H^+][A_2]}{[N]} = \frac{[H^+][A]}{[N]} f_2 = K_a f_2 \tag{4b}$$

Thus, the overall K_a is calculated from a site-specific K_a^i as

$$K_a = \frac{K_a^1}{f_1} = \frac{K_a^2}{f_2} \tag{5}$$

That is, the overall pK_a value is calculated from a site-

Scheme 3. Extended Model for the Calculation of Overall pK_a from Site-Specific Values

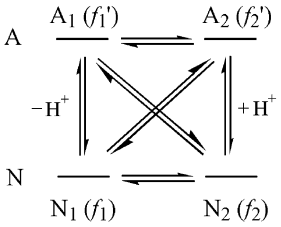

specific pK_a value (pK_a^i) as

$$pK_a = pK_a^1 + \log f_1 = pK_a^2 + \log f_2 \quad (6)$$

where $\log f_1 \leq 0$ and $\log f_2 \leq 0$.

For the special case of a deprotonated state consisting of two degenerate tautomers [$\Delta G_1 = \Delta G_2$, $f_1 = f_2 = 0.5$], eq 6 reduces to

$$pK_a = pK_a^1 - \log 2 \quad (7)$$

Multiplying eq 7 by $2.303RT$ leads this to eq 8:

$$\Delta G^\circ_{deprot} = \Delta G^\circ_1 - RT \ln 2 \quad (8)$$

as expected from a 2-fold degeneracy (*24*).

For the case where both the protonated state and the deprotonated state consist of several tautomers with fractions f_i at the protonated state and f'_j at the deprotonated state (Scheme 3), eq 4 for a site-specific dissociation constant becomes

$$K_a^{ij} = \frac{[H^+][A_j]}{[N_i]} = \frac{[H^+][A]f'_j}{[N]f_i} = K_a \frac{f'_j}{f_i} \quad (9)$$

corresponding to the deprotonation from an *i*th tautomer to a *j* ′th tautomer. The overall K_a is written as

$$K_a = K_a^{11}\frac{f_1}{f'_1} = K_a^{12}\frac{f_1}{f'_2} = K_a^{21}\frac{f_2}{f'_1} = \ldots = K_a^{ij}\frac{f_i}{f'_j} \quad (10)$$

with the overall pK_a given by

$$pK_a = pK_a^{ij} - \log f_i + \log f'_j \quad (11)$$

2.2. Calculation of a Site-Specific pK_a. A site-specific pK_a of an acid HA is given by (*25*, *26*)

$$pK_a = \frac{1}{2.303RT}\Delta G^\circ_{deprot,aq} \quad (12)$$

where R is the gas constant and T is temperature. The standard free energy of deprotonation from one of the deprotonation sites of HA in water, $\Delta G^\circ_{deprot,aq}$, is defined as (Scheme 4)

Scheme 4. Thermodynamic Cycle Used in the Calculation of a Site-Specific pK_a (*25*, *26*)

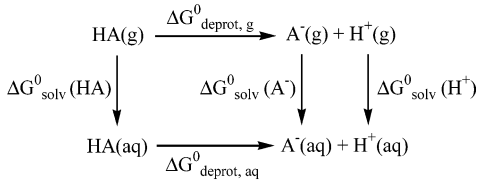

$$\Delta G^\circ_{deprot,aq} = \Delta G^\circ_{aq}(A^-) + \Delta G^\circ_{aq}(H^+) - \Delta G^\circ_{aq}(HA) \quad (13)$$

The standard free energy of each species (HA, A^-, and H^+) in water, ΔG°_{aq}, can be written by the sum of the gas-phase standard free energy ΔG°_g and the standard free energy of solvation in water ΔG°_{solv}:

$$\Delta G^\circ_{aq} = \Delta G^\circ_g + \Delta G^\circ_{solv} \quad (14)$$

2.3. Gas-Phase Free Energies. The standard free energy of each species in the gas phase, ΔG°_g, is obtained by

$$\Delta G^\circ_g = E_{0K} + ZPE + \Delta\Delta G_{0\rightarrow 298K} \quad (15)$$

The total energy of the molecule at 0 K (E_{0K}) is calculated at the optimum geometry from QM. The zero-point energy (ZPE) and the Gibbs free energy change from 0 to 298 K ($\Delta\Delta G_{0\rightarrow 298K}$) are calculated from the vibrational frequencies calculated using QM. The translational and rotational free energy contribution is also calculated in the ideal gas approximation. We used $\Delta G^\circ_g(H^+) = 2.5\,RT - T\Delta S^\circ = 1.48 - 7.76 = -6.28$ kcal/mol from the literature (*25*, *26*).

All QM calculations used the Jaguar v4.0 quantum chemistry software (*27*, *28*). To calculate the geometries and energies of the various molecules, we used density functional theory, B3LYP, which includes the generalized gradient approximation and a component of the exact Hartree−Fock exchange (*29*−*33*). Since calculations of vibration frequencies are generally quite time-consuming, the calculations were carried out in two steps. The 6-31G** basis set was first used to optimize the geometry and calculate the vibration frequencies. Then, the 6-31++G** basis set was used for the final geometry optimization started from the 6-31G** geometry:

$$\Delta G^\circ_g = ZPE^{6-31G^{**}} + \Delta\Delta G^{6-31G^{**}}_{0\rightarrow 298K} + E^{6-31++G^{**}}_{0K,g} \quad (16)$$

This strategy for the gas-phase calculation had been chosen in our previous work (Jang et al., unpublished results) after considering several basis sets for the calculation of gas-phase proton affinity (PA) and gas-phase basicity (GB) of guanine at 298 K, which are defined as the enthalpy change and the free energy change, respectively, during the protonation process in the gas phase (*34*):

$$PA = \Delta H^\circ_g(A^-) + \Delta H^\circ_g(H^+) - \Delta H^\circ_g(HA) \quad (17)$$

$$GB = \Delta G^\circ_g(A^-) + \Delta G^\circ_g(H^+) - \Delta G^\circ_g(HA) \quad (18)$$

Table 1. Gas-Phase Proton Affinities and Basicities of Guanine (kcal/mol) Calculated at B3LYP Level with Various Basis Sets, Which Shows the Importance of Diffuse Functions in $E_{0K,g}$ Calculation

	(a) 6-31G**	(b) 6-31++G** //6-31G**	(c) 6-31++G** /6-31G**	(d) 6-31++G**	experimental[a]
ZPE, $\Delta\Delta G_{0\rightarrow 298K}$	6-31G**	6-31G**	6-31G**	6-31++G**	
optimization	6-31G**	6-31G**	6-31++G**	6-31++G**	
$E_{0K,g}$	6-31G**	6-31++G**	6-31++G**	6-31++G**	
proton affinity	235.9	229.4	229.3	229.3	229 ± 2^a
gas-phase basicity	228.5	222.0	221.9	221.8	222 ± 2^a

[a] Experimental data from ref *34*.

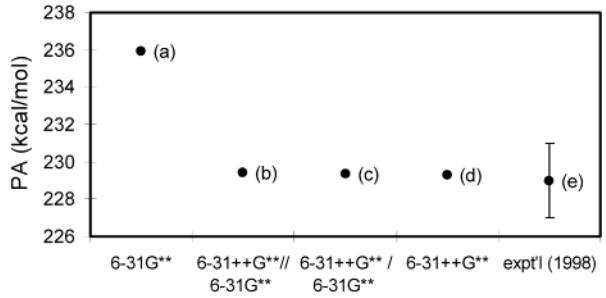

Figure 1. Gas-phase proton affinities of guanine calculated at the B3LYP level with various basis sets. This illustrates the importance of including diffuse functions in the calculation of E_{0K}.

where $\Delta H_g^\circ(H^+) = 2.5\ RT = 1.48$ kcal/mol and $\Delta G_g^\circ(H^+) = 2.5\ RT - T\Delta S^\circ = 1.48 - 7.76 = -6.28$ kcal/mol at 298 K. The four basis sets considered were (a) 6-31G** (no diffusion functions were included); (b) 6-31++G**// 6-31G** (geometry optimization and frequency calculations (i.e., ZPE and $\Delta\Delta G_{0\rightarrow 298K}$ calculation) used 6-31G** and a single-point energy calculation was done with 6-31++G** to improve E_{0K}); (c) 6-31++G**/6-31G** (preliminary geometry optimization and frequency calculation were done with 6-31G** and further geometry optimization with 6-31++G** starting from the optimum 6-31G** geometry to improve E_{0K}); and (d) 6-31++G** (diffuse functions were included in every step of calculation of E_{0K}, ZPE, and $\Delta\Delta G_{0\rightarrow 298K}$).

The results are summarized in Table 1 and Figure 1. The 6-31G** (case a) gave results very different from the others, indicating that diffuse functions are very important especially for calculation of $E_{0K,g}$. Frequency calculations were much more time-consuming than geometry optimizations, but diffuse functions had only a minor effect on those frequency calculations. Energy differences between cases c, d, and e were less than 0.2 kcal/mol, and all three results were in good agreement with experiment (*34*, *35*). Thus, the 6-31++G**/6-31G** basis set was chosen as the most efficient one for the calculations reported in this paper.

2.4. Solvation Free Energies. The standard free energies of solvation in water [ΔG_{solv}°(HA) and ΔG_{solv}°-(A^-)] were calculated using the continuum-solvation approach (*36*−*39*) by solving the Poisson−Boltzmann (PB) equation numerically (*40*). The solute was described as a low-dielectric cavity ($\epsilon_{solute} = 1$) immersed in a high-dielectric continuum of solvent [$\epsilon_{H_2O} = 80$ for water (*41*)]. The solvation process, in which a solute is transferred from a vacuum into solvent, was depicted hypothetically as two successive steps: (1) the creation of a cavity of the size of the solute in solvent and then (2) the charging of the solute to turn on the electrostatic interaction with the solvent. Therefore, the free energy of solvation (ΔG_{solv}) can be divided into two contributions: a nonelectrostatic (nonpolar) term (ΔG_{np}) and an electrostatic (polar) term (ΔG_{elec}):

$$\Delta G_{solv} = \Delta G_{elec} + \Delta G_{np} \tag{19}$$

The nonpolar contribution ΔG_{np} includes all the non-electrostatic contributions such as the energy cost of the cavity creation as well as the entropy change accompanied by the transfer of the solute from a vacuum into the solvent. It is simply treated to depend linearly on the contact area between the solute and the solvent, that is, the solvent-accessible surface area (SA) of the solute in the solution phase:

$$\Delta G_{np} = \gamma \cdot (SA) + b \tag{20}$$

The relationship had been determined for aqueous solution by Tannor and co-workers (*37*), and we used that relationship in our study without modification.

The electrostatic contribution ΔG_{elec} (*36*) corresponds to the interaction free energy (reaction field free energy) of a charge distribution inside the solute with the solvent environment of a dielectric constant $\epsilon = 80$ (for aqueous solution). This will include the screening effect of the solvent and the polarizability of the solute as well as the direct Coulombic interaction energy between them. This was calculated by solving the PB equation

$$\nabla\cdot[\epsilon(\mathbf{r})\nabla\phi(\mathbf{r})] - \epsilon(\mathbf{r})K(\mathbf{r})\sinh[\phi(\mathbf{r})] + \frac{4\pi q\rho(\mathbf{r})}{kT} = 0 \tag{21}$$

where $\phi(\mathbf{r})$ is the electrostatic potential in units of kT/q, k is the Boltzmann constant, T is the absolute temperature, q is the proton charge, $\epsilon(\mathbf{r})$ is the dielectric constant, $\rho(\mathbf{r})$ is the charge density, and $K(\mathbf{r})$ is defined as $K^2 = 8\pi q^2 I/\epsilon kT$ where I is the ionic strength. The Debye−Hückel theory is a special-case solution of the PB equation for a point charge in a medium of a uniform dielectric constant at low ionic strength. In more general cases, the solute is described as a finite-size cavity of a different dielectric constant (usually 1) from that of the solvent. For the analytic solution of the PB equation, the problem should be simplified; a simple shape of cavity should be used to represent the solute and the eq 21 should be linearized by replacing $\sinh[\phi(\mathbf{r})]$ with $\phi(\mathbf{r})$. Such models using a spherical cavity embedded with a charge or a dipole inside are the Born model and the Onsager model, respectively. These simplifications are, however, not necessary if the PB equation is solved numerically by mapping the system onto a three-dimensional grid where each grid point is assigned a value of charge, dielectric constant, and ionic strength and then calculating the electrostatic potential at each grid point. In this "finite difference PB (FDPB)" or "numerical PB" model (*36*), the electrostatic free energy

Scheme 5. Tautomers of Neutral 8-Oxoguanine Considered in This Study

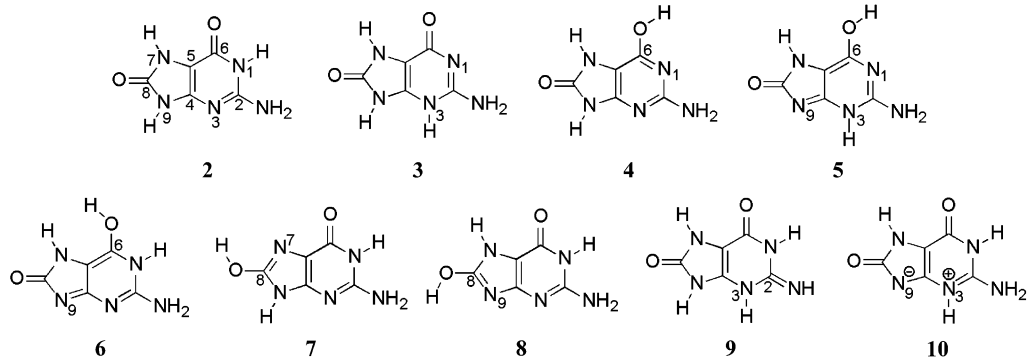

2 **3** **4** **5**

6 **7** **8** **9** **10**

Table 2. Relative Free Energies (kcal/mol) of Tautomers of Neutral 8-oxoguanine and Their Relative Boltzmann Populations in Equilibrium

	2 di-keto amine	**3** di-keto amine	**4** keto−enol amine	**5** keto−enol amine	**6** keto−enol amine	**7** keto−enol amine	**8** keto−enol amine	**9** di-keto imine	**10** di-keto amine
(a) gas phase									
$\Delta G°_{g,rel}$ [a]	0.0	16.4	0.2	18.0	29.7	13.8	11.9	13.9	29.0
population	0.6	6×10^{-13}	0.4	4×10^{-14}	1×10^{-22}	4×10^{-11}	1×10^{-9}	4×10^{-11}	3×10^{-22}
(b) aqueous phase									
$\Delta G°_{aq,rel}$ [b]	0.0	5.5	8.0	12.8	15.9	12.8	12.0	11.0	6.4
population	1.0	1×10^{-4}	1×10^{-6}	4×10^{-10}	2×10^{-12}	4×10^{-10}	2×10^{-9}	8×10^{-9}	2×10^{-5}

[a] Relative free energies with respect to $\Delta G°_g$(**2**). [b] Relative free energies with respect to $\Delta G°_{aq}$(**2**).

(ΔG_{elec}) is given by

$$\Delta G_{elec} = \frac{1}{2}\sum_i Q_i \phi(\mathbf{r}_i) \qquad (22)$$

where the sum is over the charges in the solute and $\phi(\mathbf{r}_i)$ is the electrostatic potential induced by the reaction field of the solvent medium at the site of charge *i*. The charge distribution of the solute is represented by a set of atom-centered point charges Q_i's, that is, the electrostatic-potential fitted (ESP) charges determined by the CHELP method (*42*−*44*).

The procedure is as follows. A gas-phase calculation is carried out first to obtain the ESP charges of solute atoms. On the basis of these charges, the PB equation is solved to obtain the reaction field of the solvent, which is represented as a set of polarization charges located on the solute/solvent boundary surface. The Hamiltonian is then modified to include the solute−solvent interaction due to the reaction field. This is solved to obtain a new wave function and a new set of atom-centered ESP charges. This process is repeated self-consistently until convergence (to 0.1 kcal/mol in the solvation energy), constituting the electrostatic or "polar" contribution to the solvation energy.

The solute/solvent boundary is described by the surface of closest approach as a sphere of radius 1.4 Å (probe radius for water) is rolled over the cavity of the solute, which is usually built up as a van der Waals (vdW) envelope of the solute with a chosen set of atomic radii. The atomic radii used to build the vdW envelope of the solute were 1.88 Å for sp^2-hybridized carbon, 1.46 Å for sp^2-hybridized oxygen, 1.41 Å for sp^2-hybridized nitrogen, 1.18 Å for hydrogen attached to sp^2-hybridized carbon, and 1.08 Å for other types of hydrogen, as used in our previous study (Jang et al., unpublished results). These had been reduced by 6% from the values of Marten and co-workers (*39*). In our previous study, we considered the solvation free energy of a proton in water [$\Delta G°_{solv}(H^+)$] to be a variable (Jang et al., unpublished results), since the experimental value for it remains uncertain (−254 to −264 kcal/mol) (*25*, *45*−*47*). Adjusting it for the best fit of pK_as to experimental data had led to a value (−263.47 kcal/mol) in excellent agreement with the best literature value, −263.98 kcal/mol (*47*). These parameters were used throughout all the calculations on 8-oxoguanine.

All solvation energy calculations were carried out using Jaguar v4.0 (*27*, 28) at the B3LYP/6-31++G** level, and geometry was re-optimized in solution.

2.5. Summary: Calculation Steps. Summarizing, the calculations on each species were done in three steps:

Step 1. B3LYP/6-31G**(g). Preliminary geometry optimization and frequency calculation

Step 2. B3LYP/6-31++G**(g). Final geometry optimization

Step 3. B3LYP/6-31++G**(aq). Solution-phase geometry optimization

The final standard free energy of each species in water is expressed as

$$\Delta G°_{aq} = \mathrm{ZPE}^{6-31G**} + \Delta\Delta G^{6-31G**}_{0\rightarrow 298K} + E^{6-31++G**}_{0K,g} + \Delta G°^{\,6-31++\,G**}_{solv} \qquad (23)$$

3. Results

Several tautomers of 8-oxoguanine could be present simultaneously at each ionization state, and the presence of those multiple tautomers complicates the calculation of properties regarding protonation. Thus, the free energies of all the plausible tautomers were calculated for neutral, anionic, and cationic 8-oxoguanines in gas and aqueous phases, and the proportions of the tautomers at each ionization state were estimated by the Boltzmann distribution at 298 K (sections 3.1 to 3.3), prior to the calculation of gas-phase proton affinities and basicities (section 3.4) and aqueous-phase pK_as (sections 3.5 and 3.6).

Table 3. Relative Free Energies (kcal/mol) of Tautomers of Anionic 8-Oxoguanine and Their Relative Boltzmann Populations in Equilibrium

	11$^-$	**12**$^-$	**13**$^-$	**14**$^-$	**15**$^-$	**16**$^-$
(a) gas phase						
$\Delta G°_{g,rel}$ [a]	0.0	8.0	15.3	2.3	9.5	18.7
population	0.98	1×10^{-6}	6×10^{-12}	0.02	1×10^{-7}	2×10^{-14}
(b) aqueous phase						
$\Delta G°_{aq,rel}$ [b]	0.0	1.0	3.0	7.9	9.5	12.1
population	0.84	0.16	5×10^{-3}	1×10^{-6}	1×10^{-7}	1×10^{-9}

[a] Relative energies with respect to $\Delta G°_g$(**11**$^-$). [b] Relative energies with respect to $\Delta G°_{aq}$(**11**$^-$).

Scheme 6. Tautomers of Anionic 8-Oxoguanine after the First Deprotonation

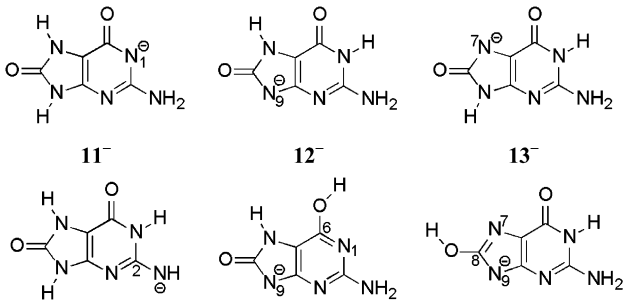

11$^-$ **12**$^-$ **13**$^-$ **14**$^-$ **15**$^-$ **16**$^-$

Scheme 7. Tautomers of Doubly Anionic 8-Oxoguanine after the Second Deprotonation

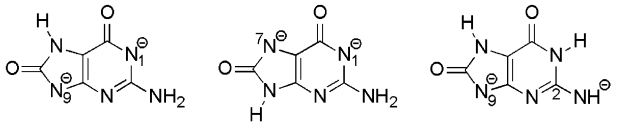

17^{2-} **18**$^{2-}$ **19**$^{2-}$

Table 4. Relative Free Energies (kcal/mol) of Doubly Anionic Tautomers Produced after the Second Deprotonation from 8-Oxoguanine and Their Relative Boltzmann Populations in Equilibrium

	17^{2-}	**18**$^{2-}$	**19**$^{2-}$
(a) gas phase			
$\Delta G°_{g,rel}$ [a]	0.7	6.9	0.0
population	0.24	7×10^{-6}	0.86
(b) aqueous phase			
$\Delta G°_{aq,rel}$ [b]	0.0	0.8	8.1
population	0.79	0.21	9×10^{-7}

[a] Relative energies with respect to $\Delta G°_g$(**19**$^{2-}$). [b] Relative energies with respect to $\Delta G°_{aq}$(**17**$^{2-}$).

3.1. Tautomers of Neutral 8-Oxoguanine. Tautomers of neutral 8-oxoguanine considered in this study (**2**−**10**) are shown in Scheme 5 and their relative free energies and relative populations in equilibrium in gas and aqueous phases are given in Table 2.

The free energy of tautomers of neutral 8-oxoguanine in the gas phase increases in the following order: **2** (6,8-diketo) ≈ **4** (6-enol-8-keto) ≪ **8** < **7** ≈ **9** ≪ **3** < **5** ≪ **10** ≈ **6**. Among the nine tautomers of neutral 8-oxoguanine, the 6,8-diketo form (**2**) and 6-enol-8-keto form produced by proton transfer from N1 to O6 (**4**) were calculated to be the most stable in the gas phase. The free energy difference between these two is only 0.2 kcal/mol. The other tautomers were found to be at least 11 kcal/mol (free energy) less stable than **2**. Thus, in equilibrium gas-phase 8-oxoguanine should exist as a mixture of **2** (60%) and **4** (40%).

In the aqueous phase, the free energy of various tautomers increases in the following order: **2** (6,8-diketo) ≪ **3** (6,8-diketo) < **10** < **4** (6-enol-8-keto) ≪ **9** < **8** < **5** ≈ **7** ≪ **6**. A 6,8-diketo tautomer **2** is predominant, as suggested previously (*9*, *12*, *18*−*23*). Other 6,8-diketo tautomers, **3** and **10**, are secondary in stability. Their free energies are 5.5 and 6.4 kcal/mol higher than **1**, making their population negligible (1×10^{-4} and 2×10^{-5}, respectively). A 6-enol-8-keto tautomer **4** is 8.0 kcal/mol higher in free energy than **1**, leading to an equilibrium proportion in aqueous solution of 1×10^{-6}.

3.2. Tautomers of Anionic 8-Oxoguanine. Tautomers of anionic 8-oxoguanine (**11**$^-$−**16**$^-$) and doubly anionic 8-oxoguanine (**17**$^{2-}$−**19**$^{2-}$) are shown in Schemes 6 and 7, respectively, and their relative free energies and relative populations in gas and aqueous phases are given in Tables 3 and 4, respectively.

Deprotonation from N_9H of 8-oxoguanine (**2**) in the gas phase results in a very unstable anionic tautomer **12**$^-$, which is 8.0 kcal/mol higher in free energy than the most stable tautomer **11**$^-$. Thus, in the gas phase, anionic 8-oxoguanine should exist almost exclusively as **11**$^-$ (98%; around 2% would be **14**$^-$ generated by deprotonation from exocyclic NH_2).

In aqueous solution **12**$^-$ becomes greatly stabilized, becoming just 1.0 kcal/mol higher in energy than **11**$^-$. Thus, anionic 8-oxoguanine in the aqueous phase should exist as a mixture of **11**$^-$ and **12**$^-$ (84% and 16%, respectively, in equilibrium).

3.3. Tautomers of Cationic 8-Oxoguanine. Tautomers of cationic 8-oxoguanine considered in this study are shown in Scheme 8, and their relative free energies and relative populations in gas and aqueous phases are given in Table 5.

The N7 site, which is the major protonation site for guanine (Jang et al., unpublished results), is not available in 8-oxoguanine, since it is protonated already in its neutral state. Instead, O6 is exclusively protonated (**21**$^+$) in the gas phase and N3 is exclusively protonated (**20**$^+$) in the aqueous phase.

3.4. Gas-Phase Proton Affinity and Basicity. Assuming slow equilibration between tautomers in the gas phase, a series of PA and GB were calculated (eqs 17 and 18), each of which corresponds to protonation from a major tautomer of neutral 8-oxoguanine (**2** or **4**) to a major accessible tautomer of cationic 8-oxoguanine (Scheme 9 and Table 6).

3.5. pK_a. Assuming a rapid equilibrium between tautomers in the aqueous phase, the overall pK_a value was calculated from a site-specific value (pK_a^{ij}), which corresponds to a deprotonation from the *i*th tautomer to the *j*th tautomer at the deprotonated state (eq 11). The relative populations of those tautomers (f_i and f'_j) were calculated from the Boltzmann distribution in sections 3.1−3.3 (Tables 2−5). The site-specific pK_a (pK_a^{ij}) was calculated from the free energy of deprotonation of the corresponding process (eq 12).

Scheme 8. Tautomers of Cationic 8-Oxoguanine Considered in This Study

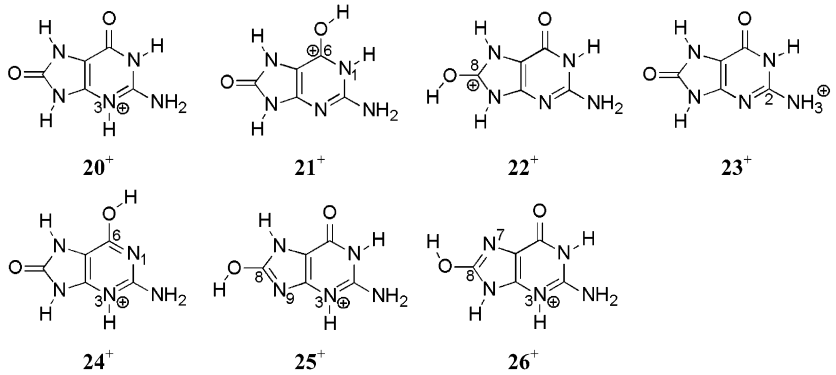

Table 5. Relative Free Energies (kcal/mol) of Tautomers of Cationic 8-oxoguanine and Their Relative Boltzmann Populations in Equilibrium

	20$^+$	**21**$^+$	**22**$^+$	**23**$^+$	**24**$^+$	**25**$^+$	**26**$^+$
(a) gas phase							
$\Delta G°_{g,rel}$ [a]	7.8	0.0	4.4	30.1	6.9	3.7	15.6
population	2×10^{-6}	1.0	6×10^{-4}	8×10^{-23}	9×10^{-6}	2×10^{-3}	3×10^{-12}
(b) aqueous phase							
$\Delta G°_{aq,rel}$ [b]	0.0	6.2	10.0	7.0	7.9	8.8	11.3
population	1.0	3×10^{-5}	5×10^{-8}	7×10^{-6}	1×10^{-6}	3×10^{-7}	5×10^{-9}

[a] Relative energies with respect to $\Delta G°_g$(**21**$^+$). [b] Relative energies with respect to $\Delta G°_{aq}$(**20**$^+$).

Scheme 9. Series of Gas-Phase Basicities (GB; kcal/mol) of 8-Oxoguanine[a]

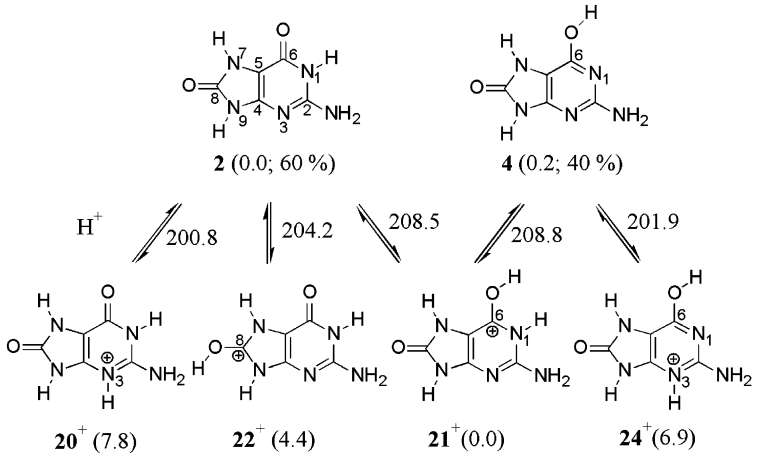

[a] Relative free energies (kcal/mol) of tautomers at each ionization state are shown in parentheses together with the relative population.

Table 6. Gas-Phase Proton Affinities (PA) and Basicities (GB) of 8-Oxoguanine (kcal/mol)

	calculation
PA	214.9 (**2**→**21**$^+$; O6), 211.4 (**2**→**22**$^+$; O8), 207.5 (**2**→**20**$^+$; N3)
	215.1 (**4**→**21**$^+$; N1), 208.5 (**4**→**24**$^+$; N3)
GB	208.5 (**2**→**21**$^+$; O6), 204.2 (**2**→**22**$^+$; O8), 200.8 (**2**→**20**$^+$; N3)
	208.8 (**4**→**21**$^+$; N1), 201.9 (**4**→**24**$^+$; N3)

Calculated pK_a values of 8-oxoguanine are summarized in Scheme 10 and Table 7. According to the calculation, the pK_{a1} of 8-oxoguanine (0.2) is much lower than that of guanine (3.2), because the best protonation site (N7) in neutral guanine is not available for protonation in neutral 8-oxoguanine. Instead, the N3 site is first protonated for 8-oxoguanine. The pK_{a2} of 8-oxoguanine is calculated to be 8.7, which is 0.7 unit lower than that of guanine (9.4). The predominant protonation site involved is N_1H both in guanine and in 8-oxoguanine. Thus N_1H is more acidic in 8-oxoguanine than in guanine. The pK_{a3} of 8-oxoguanine (11.9) is lower than that of guanine (12.6), with the same protonation site, N_9H, in both cases. These calculated results agree with experiments on the nucleoside analogues 8-oxoguanosine and 8-oxodeoxyguanosine (*20*), discussed below in section 4.2.

3.6. pK_a Estimated with a Proton Kept at N9. In nucleosides or in DNA, the N9 of 8-oxoguanine is connected to a sugar rather than a proton and cannot participate in deprotonation. Thus, to clarify the discussions in the next sections, we want to consider only the tautomers with a proton at N9 (Scheme 11 and Table 8), as models of the corresponding nucleoside. With a proton kept at N9, 8-oxoguanine exists predominantly as a single tautomer at each ionization state. Thus, the neutral species exist as a diketo form **2**. Protonation occurs predominantly at N3 (pK_{a1} = 0.22). Deprotonation occurs exclusively at N_1H (pK_{a2} = 8.76) and then at N_7H (pK_{a3} = 12.53). The new values will be used in the discussions in the following sections.

4. Discussion

4.1. Tautomerism of 8-Oxoguanine. Our calculations (Scheme 5 and Table 2) show that the 6,8-diketo tautomer, **2,** is the most stable in aqueous phase, indicat-

Scheme 10. Major Tautomers of 8-Oxoguanine at Each Ionization State in the Aqueous Phase and Calculated pK_a Values

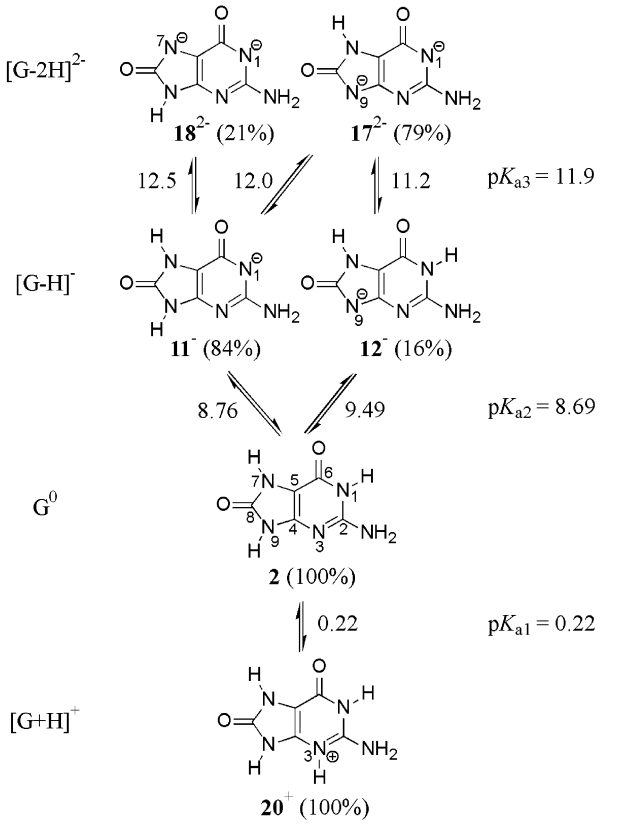

Table 7. Calculated pK_a Values and the Corresponding Protonation Sites

	calculation	experiment[d]	experiment[f]
(a) guanine			
pK_{a3}[a]	12.61 (N9)	12.3−12.4	
pK_{a2}[b]	9.44 (N1)	9.2−9.6[e]	9.2
pK_{a1}[c]	3.15 (N7)	3.2−3.3[e]	1.6−2.1
(b) 8-oxoguanine			
pK_{a3}[a]	11.93 (N9)		11.2 (11.7)[g]
pK_{a2}[b]	8.69 (N1)		8.5 (8.6)[g]
pK_{a1}[c]	0.22 (N3)		∼0.1

[a] From $\Delta G°_{deprot,aq} = \Delta G°_{aq}$ ($[G-2H]^{2-}$) + $\Delta G°_{aq}$ (H^+) − $\Delta G°_{aq}$ ($[G-H]^-$). [b] From $\Delta G°_{deprot,aq} = \Delta G°_{aq}$ ($[G-H]^-$) + $\Delta G°_{aq}$ (H^+) − $\Delta G°_{aq}$ (G). [c] From $\Delta G°_{deprot,aq} = \Delta G°_{aq}$ (G) + $\Delta G°_{aq}$ (H^+) − $\Delta G°_{aq}$ ($[G+H]^+$). [d] Experimental values for guanine base (*58*−*64*). [e] The values measured at 40 °C are 9.92 (pK_{a2}) and 3.22 (pK_{a1}) (*61*, *64*). [f] Experimental values for nucleosides, guanosine (*59*, *62*, *63*) and 8-oxoguanosine (*20*). [g] Experimental values for 8-oxodeoxyguanosine (*20*).

ing that it would be a dominant species under physiological conditions, as suggested elsewhere (*9*, *12*, *18*−*23*). The next available tautomers are **3** (with the N_1 proton transferred to N_3), **10** (with the N_9 proton transferred to N_3), and **4** (in a 6-enol-8-keto form). They are 5.5, 6.4, and 8.0 kcal/mol higher in free energy than **2**, respectively. Formation of **4** would directly affect the hydrogen bonding scheme of 8-oxoguanine, but it would exist at a frequency of approximately 1×10^{-6}. This is twice as large as the relative population of the 6-enol tautomers of guanine (5×10^{-7}) under the same conditions.

The tautomeric form of 8-oxoguanine has been investigated in several previous computational studies (*21*−*23*). Despite differences in computational details, all studies converge on the conclusion that the diketo form (**2**) of 8-oxoguanine will predominate under physiological conditions.

4.2. pK_a of 8-Oxoguanine: Comparison with Experiment. The pK_a values of 8-oxoguanosine and 8-oxodeoxyguanosine have been determined from the pH dependence of their ^{13}C NMR (*20*) or ^{15}N NMR (*19*) spectra in water at ambient temperature. The values determined for 8-oxoguanine are 8.5 (pK_{a2}) and 11.2 (pK_{a3}). Around pH 8.5, large chemical shift changes of C6 and C2 accompanying removal of a proton from N_1 were observed, indicating keto-to-enolate conversion at C6. Around pH 11.2, the same shift occurs at C8 and C5 due to the second ionization at N7 followed by keto-to-enolate conversion at C8. The pH-dependent water solubility of 8-oxoguanosine increases dramatically at extremes of pH and becomes minimal at neutral pH, indicating that the species is neutral around pH 6. No significant spectral change was observed in the pH range 1−6. The solubility improved slightly at pH ∼0.1. At this pH, C4 and C2, which are located α to N3, were shielded. This implies that only the pyridine-type N3 becomes slightly protonated at extremely acidic pH. The corresponding values of 8-oxodeoxyguanosine were determined as 8.6 and 11.7.

Our calculations on the ionization of 8-oxoguanine are in accord with experimental studies on 8oxoG nucleoside analogues. The calculated protonation sites are in agreement with experimental data in that the first deprotonation occurs predominantly from N_1H, that the second occurs from the five-membered imidazole ring (from N_9H for 8-oxoguanine and from N_7H for 8-oxoguanosine since N9 is connected to sugar), and that protonation occurs on N3 only very slightly even at low pH. Ionization in either the N1 or N7 positions results in substantial charge delocalization onto nearby heteroatoms. The calculated geometrical parameters also show the same trends (Table 9).

4.3. Dipole Moment. The static dipoles of guanine and 8-oxoguanine differ by 42°, as indicated in Figure 2. In the anti conformation of 8oxoG, there is considerable repulsion between the 8-oxo position and O4′ of the deoxyribose. This repulsion can be reduced by rotation of 8-oxoguanine toward the helix axis as shown in Figure 3 (calculation details are in section 4.4). Interestingly, such rotation would bring the static dipole of 8-oxoguanine into a position similar to that of guanine in the native state. When in this position, 8oxoG would present a hydrogen bonding face similar to that seen when the 8oxoG is in the syn conformation. The potential implications of this conformation have not been addressed experimentally.

4.4. Glycosidic Torsion Preference. We also investigated how the change in glycosidic preference might lead to 8oxoG·A mispairing. This has been proposed to be the most important factor in causing mispairing (*3*, *8*, *9*). We studied the glycosidic torsion preferences of guanine and 8-oxoguanine residues by calculating the relative energies of anti and syn conformers for a fragment of a single-strand DNA containing guanine or 8-oxoguanine. The model fragments, 2′-deoxyguanosine-3′,5′-bisphosphate (pdGp) and 2′-deoxy-8-oxoguanosine-3′,5′-bisphosphate (p8oxodGp), are shown in Figure 3. The terminal hydrogens of both phosphate groups ($-PO_3H$) were replaced with methyl groups. Due to the size of the molecules, the calculations utilized a lower

Scheme 11. pK_a Values Calculated for a Simple Model of Guanine (a) and 8-Oxoguanine (b) in DNA[a]

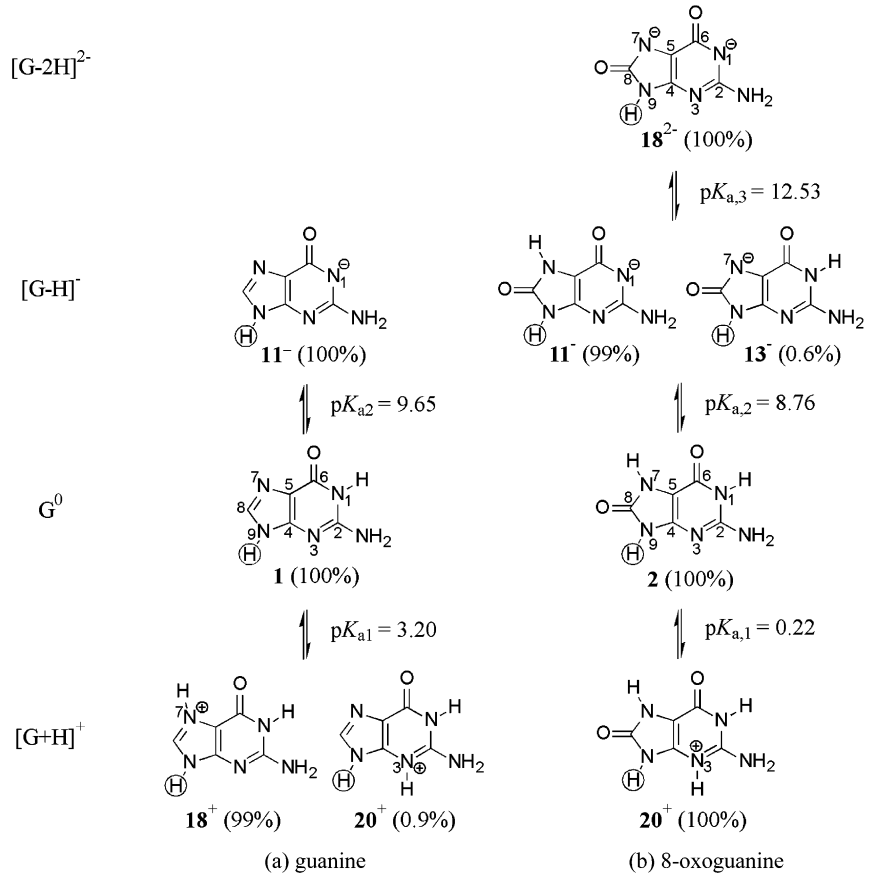

[a] The proton on N9 represents the deoxyribose unit and is not involved in deprotonation.

Table 8. pK_a Values Estimated with a Proton Kept at N9 and the Corresponding Protonation Sites

	(a) guanine	(b) 8-oxoguanine
pK_{a3}		12.53 (N7)
pK_{a2}	9.65(N1)	8.76 (N1)
pK_{a1}	3.20(N7)	0.22 (N3)
pK_{a2} (N9)[a]	10.03	9.49

[a] pK_{a2} corresponding to the deprotonation from N_9H of neutral species.

Table 9. Calculated Geometrical Parameters (bond length in angstroms and inversion of exocyclic $-NH_2$ group in degrees) of 8-Oxoguanine and Their Changes during the First and Second Deprotonations[a]

	2	**11^-**	**18^{2-}**		**2**	**11^-**	**18^{2-}**
N_1-C_2	**1.37**	**1.34**	1.34	C_5-N_7	1.40	1.40	1.39
C_2-N_3	**1.33**	**1.35**	1.34	**N_7-C_8**	1.37	**1.37**	**1.34**
N_3-C_4	1.35	1.34	1.35	C_8-N_9	1.39	1.39	1.40
C_4-C_5	1.38	1.38	1.38	N_9-C_4	1.37	1.38	1.38
C_5-C_6	1.41	1.41	1.41	**C_8-O_8**	1.24	**1.24**	**1.27**
C_6-N_1	**1.41**	**1.38**	1.38				
C_6-O_6	**1.25**	**1.27**	1.28				
C_2-N_2	**1.35**	**1.38**	**1.39**				
$-NH_2$	**21.9**	**36.5**	42.0				

[a] Significant changes are presented in bold faces.

level of density functional theory. The geometry was optimized in the gas phase with the 6-31G* basis set. At this geometry, a single-point calculation was done with the 6-31+G* basis set in gas phase to improve the gas-phase energy (E_{0K}), and another single-point energy calculation was done in aqueous phase with the 6-31G* basis set to obtain the solvation energy (ΔG_{solv}). The frequency calculations for ZPE's and thermodynamic corrections ($\Delta\Delta G_{0\rightarrow 298K}$) were omitted, presuming that these quantities would be similar for two conformations. This simpler sequence of calculation steps is then:

Step 1. B3LYP/6-31G*(g) for geometry optimization

Step 2. B3LYP/6-31+G*(g) for single-point energy calculation ($E_{0K}^{6-31+G*//6-31G*}$)

Step 3. B3LYP/6-31G*(aq) for single-point solvation energy calculation (ΔG_{solv}^{6-31G*})

$$\Delta G_{aq}^{o} = E_{0K,g}^{6-31+G*//6-31G*} + \Delta G_{solv}^{o\ 6-31G*} \qquad (24)$$

The optimized structures of syn and anti conformers are shown in Figure 3 and their relative energies are listed in Table 10.

The syn conformer of 8oxoG is highly preferred. In the anti conformation, considerable repulsion occurs between O8 of 8oxoG and the backbone oxygens—O4′ of the sugar and O5′ of the phosphate. When in the syn conformation, these repulsive interactions are considerably reduced. The distance between O8 of 8oxoG and the nearest oxygen increases to at least 4 Å. The RMS deviation of positions of common atoms between G (anti) and 8oxoG (anti) is as large as 1.03 Å. In contrast, the corresponding RMS deviation between G (syn) and 8oxoG (syn) is only 0.12 Å. That is, there was only a small change in the syn conformation after replacing H8 of G with O8 of 8oxoG, because the only repulsive interaction in the case of 8oxoG (syn) would be between O8 and another O5′ which are separated from each other by >5 Å (marked as a line in Figure 3, panels c and d). Moreover, in the syn conformation there is an attractive interaction between

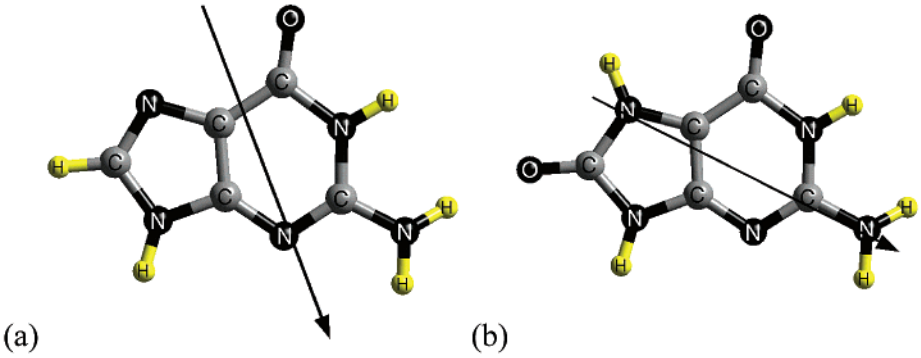

Figure 2. Optimized structure and dipole moment vector of the most stable tautomer of the neutral species. (a) Guanine and (b) 8-oxoguanine. The 8-oxoguanine should be rotated clockwise by 42° to match its dipole moment orientation to that of guanine.

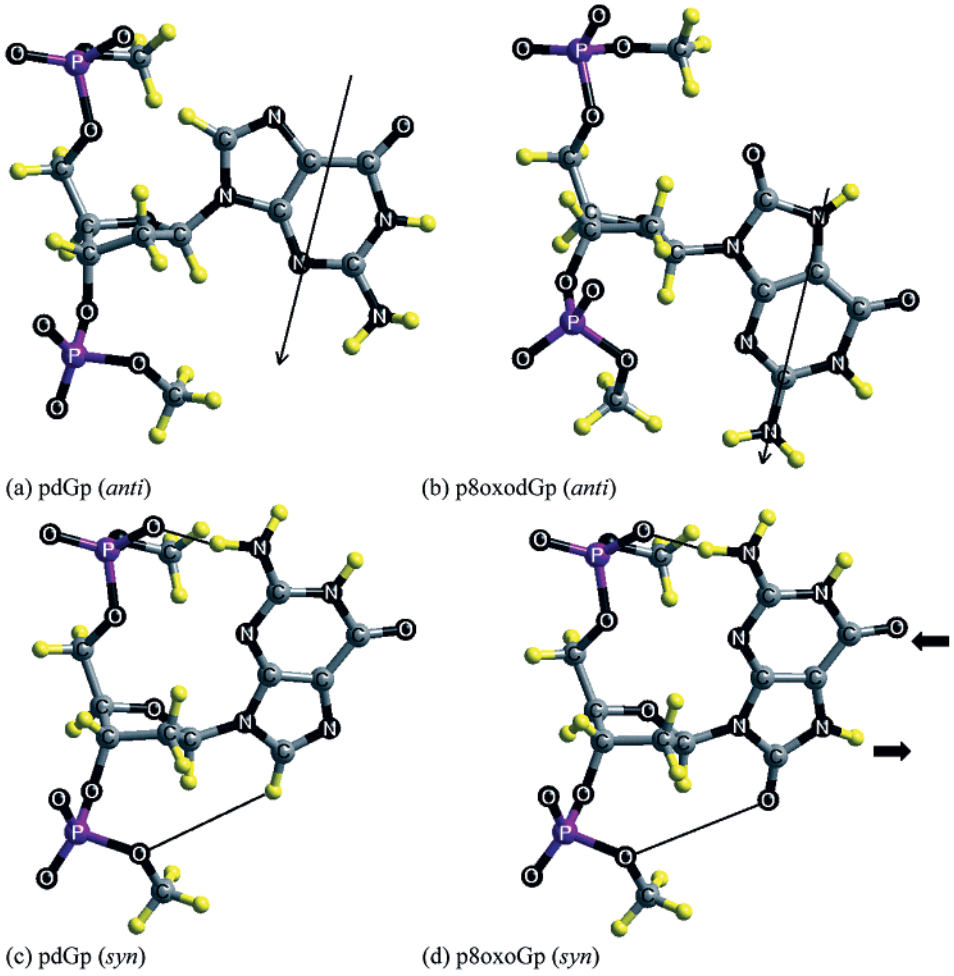

Figure 3. Optimized structure of a fragment of a single DNA strand containing guanine (a, c) or 8-oxoguanine (b, d). In panel b, the repulsion between O8 of the 8-oxoguanine base and the O5′ of the ribose backbone induces a change of orientation of the molecular plane of the base. After this rotation the dipole moment orientation of 8-oxoguanine base matches that of the original guanine, presumably allowing the maximum of base stacking interaction. The dipole moment orientations shown here are approximately taken from those of guanine and 8-oxoguanine bases shown in Figure 2.

O5′ and exocyclic NH_2 moiety, which are within 1.7 Å (marked as another line in Figure 3, panels c and d).

Although we show that 8oxoG prefers the syn conformation, it is not obvious that the anti-to-syn conversion would be favorable in 8oxodGTP. Furthermore, the favorability would be especially uncertain in DNA, due to base stacking. Thus, we are planning to investigate the torsion barrier in 8oxodGTP and in a single-strand DNA using quantum mechanics and force-field methods.

4.5. Recognition and Repair of 8oxoG. It is estimated that several hundred 8oxoG residues are formed daily in human cells (*48*). The number can be increased substantially under oxidative stress or radiation exposure (*49*−*52*). Despite this substantial number of damaged bases per cell per day, the 8oxoG residues are distributed among 10^9 undamaged bases. How do DNA repair enzymes locate damaged bases, and how are they distinguished from undamaged bases? DNA polymerases only make mistakes at a frequency of one error every 10^3 to 10^5 bases (*53*). In contrast to polymerases, the repair enzyme hOgg1 must find 8oxoG residues and remove them with considerably greater fidelity, as hOgg1 would

Scheme 12. Resonance Structures after the First Deprotonation from 8-Oxoguanosine[a]

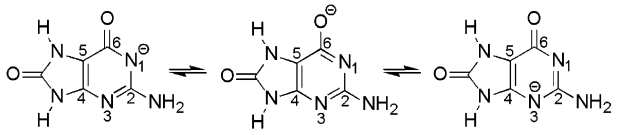

[a] Similar resonance occurs on 5-membered imidazoline ring after second deprotonation.

Table 10. Relative Energies (kcal/mol) of syn and anti Conformers of a Fragment of a Single-Stranded DNA Containing (a) Guanine or (b) 8-Oxoguanine

	anti	syn	anti/syn preference
(a) guanine (kcal/mol)	0.33	0.00	slight preference for *syn*
(b) 8-oxoguanine (kcal/mol)	6.87	0.00	*syn* highly preferred
RMS deviation of positions of common atoms between a and b (Å)	1.03	0.12	

fragment the human genome if it removed normal guanine residues at a frequency of 1 in 10^5. The mechanisms by which the repair enzymes generate such high selectivity are not well understood.

One characteristic distinguishing guanine and 8-oxoguanine is the N7 proton of 8-oxoguanine. Although 8-oxoguanine is commonly referred to as 8-hydroxyguanine (**7**), our studies show that the 8-oxo tautomer (**2**) predominates in the gas phase and in water. We have investigated the energy cost of moving this proton via tautomerization or ionization, as summarized for aqueous phase in Table 11. Indeed, removal of the proton at the N7 position of 8-oxoguanine requires substantial energy whether transferring the proton to the 8-oxygen (**2** → **7**; 12.8 kcal/mol in aqueous phase) or ionizing and transferring the proton to solvent (**2** → **13**$^-$; 5.4 kcal/mol in aqueous phase at pH 7). Structural studies of 8oxoG

Table 11. Free Energy Costs (kcal/mol) of 8-Oxoguanine Configurations over the Most Stable Configuration 2 under Physiological Conditions (aqueous solution at pH 7 and 298 K)

neutral	**3**	**4**	**5**	**6**	**7**	**8**	**9**	**10**
$\Delta\Delta G°_{aq,pH7}$ [a]	5.5	8.0	12.8	15.9	12.8	12.0	11.0	6.4
deprotonated	**11**$^-$	**12**$^-$	**13**$^-$	**14**$^-$	**15**$^-$	**16**$^-$		
$\Delta\Delta G°_{aq,pH7}$ [b]	2.4	3.4	5.4	10.3	11.9	14.5		
doubly deprotonated	**17**$^{2-}$	**18**$^{2-}$	**19**$^{2-}$					
$\Delta\Delta G°_{aq,pH7}$ [c]	9.2	9.9	17.2					
protonated	**20**$^+$	**21**$^+$	**22**$^+$	**23**$^+$	**24**$^+$	**25**$^+$	**26**$^+$	
$\Delta\Delta G°_{aq,pH7}$ [d]	9.2	15.4	19.2	16.3	17.2	18.1	20.6	

[a] $\Delta\Delta G°_{aq,pH7}(\mathbf{X}) = \Delta G°_{aq}(\mathbf{X}) - \Delta G°_{aq}(\mathbf{2})$. [b] $\Delta\Delta G°_{aq,pH7}(\mathbf{X}^+) = \Delta G°_{aq}(\mathbf{X}^+) - [\Delta G°_{aq}(H^+) + RT \ln 10^{-7}] - \Delta G°_{aq}(\mathbf{2})$. [c] $\Delta\Delta G°_{aq,pH7}(\mathbf{X}^-) = \Delta G°_{aq}(\mathbf{X}^-) + [\Delta G°_{aq}(H^+) + RT \ln 10^{-7}] - \Delta G°_{aq}(\mathbf{2})$. [d] $\Delta\Delta G°_{aq,pH7}(\mathbf{X}^{2-}) = \Delta G°_{aq}(\mathbf{X}^{2-}) + 2[\Delta G°_{aq}(H^+) + RT \ln 10^{-7}] - \Delta G°_{aq}(\mathbf{2})$, where $\Delta G°_{aq}(H^+) + RT \ln 10^{-7} = -269.75 - 9.54 = -279.29$ (kcal/mol).

complexed with hOgg1 indicate formation of a hydrogen bond between the enzyme and the N7 8oxoG proton, suggesting the importance of this interaction (*14*). We conclude that this proton remains at the N7 position and would thus serve as an important landmark for distinguishing guanine and 8-oxoguanine.

The mechanism by which hOgg1 catalyzes base removal is less clear. We investigated several pathways by which the proton at the N9 position of 8-oxoguanine, which forms the scissile bond of the corresponding deoxynucleoside, might be removed (Scheme 13). The pK_a of the N9 proton, as determined in this study (9.5; **2** → **12**$^-$ in Scheme 10), is somewhat lower than that of guanine (10.0; Jang et al., unpublished results). The enhanced stability of a negative charge at the N9 position would potentially facilitate glycosidic bond cleavage. Recently, Karplus and co-workers (*54*) have proposed an N1 ionized uracil intermediate in the enzymatic removal of uracil by uracil−DNA glycosylase, consistent with experimental findings (*55*). However, the pK_a difference

Scheme 13. Configurations of 8oxoG That Might Be Involved in Glycosylase-Mediated 8oxoG Removal[a]

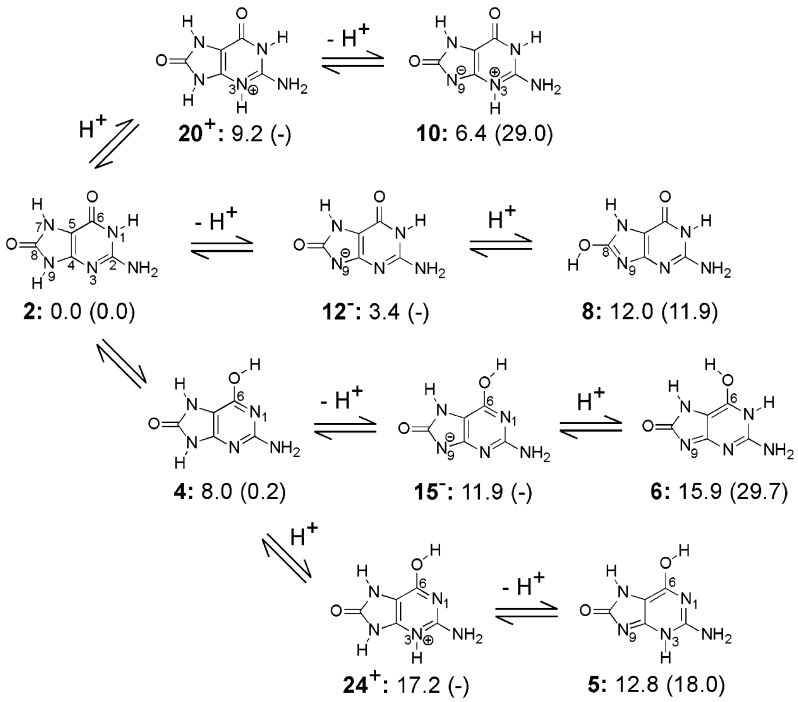

[a] Numbers below the figures are the energy cost in kcal/mol of that configuration over the most stable configuration under physiological conditions. Numbers in parentheses are the gas phase values.

between guanine and 8-oxoguanine is small, and would provide little additional stabilization.

The lowest lying higher energy tautomeric form is the 6-enol tautomer (**4**). Indeed, in the gas phase, the 6-keto (**2**) and 6-enol (**4**) tautomers are of similar energy (0.2 kcal/mol difference; Table 2). Potentially, trapped water molecules and amino acid residues in the glycosylase active site could promote formation of this tautomer. We investigated if a shift to this form would increase the acidity of the N9 proton (**4** → **15**$^-$ in Scheme 13) or promote a shift of the N9 to the N3 position (**4** → **5** in Scheme 13). However, these changes provided minimal stabilization for the repair intermediate [3.9 kcal/mol for **4** (6-enol) → **15**$^-$ as opposed to 3.4 kcal/mol for **2** (6-keto) → **12**$^-$ and 4.8 kcal/mol for **4** (6-enol) → **5** as opposed to 6.4 kcal/mol for **2** (6-keto) → **10**; Scheme 13].

The most likely site of protonation of 8-oxoguanine is the N3 position. However, the N3 nitrogen is not very basic, with a pK_a of 0.22. In the mechanism proposed by Verdine and others, lysine 249 must first be deprotonated prior to attacking the C1 position (*14*, *56*, *57*). They propose that a nearby aspartic acid residue might participate in lysine deprotonation. Alternatively, the N3 position of 8oxoG might act as the proton acceptor. Protonation of the N3 position of 8oxoG substantially increases the acidity of the N9 position in either the keto or enol forms [−2.8 kcal/mol for **20**$^+$ (6-keto cation) → **10** and −4.4 kcal/mol for **24**$^+$ (6-enol cation) → **5** as opposed to 3.4 kcal/mol for **2** (neutral) → **12**$^-$; Scheme 13]. It has been proposed by Karplus et al. that the O2 position of uracil participates in the delocalization of the N1 charge on uracil, facilitating the action of uracil-DNA glycosylase (*54*). Perhaps the N3 position of purines could similarly act in facilitating glycosylase removal.

Summary

The tautomeric configurations and ionized forms of 8-oxoguanine were investigated using first principles quantum mechanics (density functional theory, B3LYP, in combination with the Poisson−Boltzmann continuum-solvation model). We show that the major tautomer of neutral 8-oxoguanine in aqueous solution is the 6,8-diketo form **2** and that the 6-enol-8-keto tautomer **4** is 8.0 kcal/mol higher in free energy in water, implying a relative population of 1×10^{-6} under physiological conditions. Instead, the increased acidity at N1 due to oxidation at C8 results in an increased population of deprotonated 8-oxoguanine **9**$^-$ at neutral pH (around 1% at pH 7 and around 10% at pH 8), modifying its hydrogen-bond characteristics. Loss of the N1 proton would destabilize the normal guanine-cytosine pair, promoting formation of aberrant base pairs.

From calculations on 2′-deoxyguanosine-3′,5′-bisphosphate and its 8-oxo analogue, we find that the repulsion between the O8 of 8-oxoguanine and nearby sugar and phosphate oxygen atoms induces a rotation of the 8-oxoguanine plane (Figure 3b) or a torsional switch around its glycosidic bond (anti-to-syn; Figure 3d). In either case, this would change its hydrogen-bond characteristics and potentially promote mispairing.

The N7 proton of 8-oxoguanine is difficult to remove either through tautomerization or ionization, consistent with its involvement as an important landmark distinguishing guanine from 8-oxoguanine. We searched for additional properties that might allow discrimination between guanine and 8-oxoguanine, but none were found. Catalysis of glycosylase-mediated glycosidic bond cleavage might involve protonation of the N3 position. However, the energy cost of protonation at this site is similar for both bases. Additional studies are in progress to understand how the active site might facilitate the fidelity and rate of damaged base removal.

Acknowledgment. This work was supported in part by the National Institutes of Health [HD36385 (W.A.G), GM 41336 (L.C.S.), and CA 85779 (L.C.S. and W.A.G.)], the BK21 program and the CMC of Korea (Y.H.J., S.H., and D.S.C.). The computations were aided by an SUR grant from IBM. In addition, the facilities of the MSC are also supported by DOE-ASCI, ARO-MURI, ARO-DURIP, National Science Foundation [CHE-99-85574 and 99-77872], Dow Chemical, 3M, Beckman Institute, Avery-Dennison, Chevron Corporation, Seiko Epson, Asahi Chemical, and Kellogg's.

References

(1) Kasai, H., and Nishimura, S. (1984) Hydroxylation of deoxyguanosine at the C-8 position by ascorbic-acid and other reducing agents. *Nucleic Acids Res.* **12**, 2137−2145.

(2) Kuchino, Y., Mori, F., Kasai, H., Inoue, H., Iwai, S., Miura, K., Ohtsuka, E., and Nishimura, S. (1987) Misreading of DNA templates containing 8-hydroxydeoxyguanosine at the modified base and at adjacent residues. *Nature* **327**, 77−79.

(3) Grollman, A. P., and Moriya, M. (1993) Mutagenesis by 8-oxoguanine: an enemy within. *Trends Genet.* **9**, 246−249.

(4) Shibutani, S., Takeshita, M., and Grollman, A. P. (1991) Insertion of specific bases during DNA synthesis past the oxidation-damaged base 8-oxodG. *Nature* **349**, 431−434.

(5) Wood, M. L., Dizdaroglu, M., Gajewski, E., and Essigmann, J. M. (1990) Mechanistic studies of ionizing radiation and oxidative mutagenesis: Genetic effects of a single 8-hydroxyguanine (7-hydro-8-oxoguanine) residue inserted at a unique site in a viral genome. *Biochemistry* **29**, 7024−7032.

(6) Moriya, M., Ou, C., Bodepudi, V., Johnson, F., Takeshita, M., and Grollman, A. P. (1991) Site-specific mutagenesis using a gapped duplex vector: A study of translesion synthesis past 8-oxodeoxyguanosine in *E. coli*. *Mutat. Res.* **254**, 281−288.

(7) Cheng, K. C., Cahill, D. S., Kasai, H., Nishimura, S., and Loeb, L. A. (1992) 8-Hydroxyguanine, an abundant form of oxidative DNA damage, causes G→T and A→C substitutions. *J. Biol. Chem.* **267**, 166−172.

(8) Uesugi, S., and Ikehara, M. (1977) Carbon-13 magnetic resonance spectra of 8-substituted purine nucleosides. Characteristic shifts for the syn conformation. *J. Am. Chem. Soc.* **99**, 3250−3253.

(9) Culp, S. J., Cho, B. P., Kadlubar, F. F., and Evans, F. E. (1989) Structural and conformational analyses of 8-hydroxy-2′-deoxyguanosine. *Chem. Res. Toxicol.* **2**, 416−422.

(10) Kouchakdjian, M., Bodepudi, V., Shibutani, S., Eisenberg, M., Johnson, F., Grollman, A. P., and Patel, D. J. (1991) NMR structural studies of the ionizing radiation adduct 7-hydro-8-oxodeoxyguanosine (8-oxo-7H-dG) opposite deoxyadenosine in a DNA duplex. 8-Oxo-7H-dG(syn):dA(anti) alignment at lesion site. *Biochemistry* **30**, 1403−1412.

(11) McAuley-Hecht, K. E., Leonard, G. A., Gibson, N. J., Thomson, J. B., Watson, W. P., Hunter, W. N., and Brown, T. (1994) Crystal structure of a DNA duplex containing 8-hydroxydeoxyguanine-adenine base pairs. *Biochemistry* **33**, 10266−10270.

(12) Oda, Y., Uesugi, S., Ikehara, M., Nishimura, S., Kawase, Y., Ishikawa, H., Inoue, H., and Ohtsuka, E. (1991) NMR studies of a DNA containing 8-hydroxydeoxyguanosine. *Nucleic Acids Res.* **19**, 1407−1412.

(13) Lipscomb, L. A., Peek, M. E., Morningstar, M. L., Verghis, S. M., Miller, E. M., Rich, A., Essigmann, J. M., and Williams, L. D. (1995) X-ray structure of a DNA decamer containing 7,8-dihydro-8-oxoguanine. *Proc. Natl. Acad. Sci. U.S.A.* **92**, 719−723.

(14) Bruner, S. D., Norman, D. P. G., and Verdine, G. L. (2000) Structural basis for recognition and repair of the endogenous mutagen 8-oxoguanine in DNA. *Nature* **403**, 859−866.

(15) Albert, A., and Brown, D. J. (1954) Purine studies. Part I. Stability to acid and alkali. Solubility. Ionization. Comparison with Pteridines. *J. Chem. Soc.* 2060−2071.

(16) La Francois, C. J., Jang, Y. H., Cagin, T., Goddard, W. A., III, and Sowers, L. C. (2000) Conformation and proton configuration of pyrimidine deoxynucleoside oxidation damage products in water. *Chem. Res. Toxicol.* **13**, 462−470.

(17) Jang, Y. H., Sowers, L. C., Cagin, T., and Goddard, W. A., III (2001) First principles calculation of pK_a values for 5-substituted uracils. *J. Phys. Chem. A* **105**, 274−280.
(18) Aida, M., and Nishimura, S. (1987) An ab initio molecular orbital study on the characteristics of 8-hydroxyguanine. *Mutat. Res.* **192**, 83−89.
(19) Cho, B. P., Kadlubar, F. F., Culp, S. J., and Evans, F. E. (1990) ^{15}N nuclear magnetic resonance studies on the tautomerism of 8-hydroxy-2′-deoxyguanosine, 8-hydroxyguanosine, and other C8-substituted guanine nucleosides. *Chem. Res. Toxicol.* **3**, 445−452.
(20) Cho, B. P. (1993) Structure of oxidatively damaged nucleic acid adducts: pH dependence of the ^{13}C NMR spectra of 8-oxoguanosine and 8-oxoadenosine. *Magn. Reson. Chem.* **31**, 1048−1053.
(21) Venkateswarlu, D., and Leszczynski, J. (1998) Tautomeric equilibria in 8-oxopurines: Implications for mutagenicity. *J. Comput.-Aided Mol. Des.* **12**, 373−382.
(22) Gu, J., and Leszczynski, J. (1999) Influence of the oxygen at the C8 position on the intramolecular proton transfer in C8-oxidative guanine. *J. Phys. Chem. A* **103**, 577−584.
(23) Cysewski, P. (1998) An ab initio study of the tautomeric and coding properties of 8-oxo-guanine. *J. Chem. Soc., Faraday Trans.* **94**, 3117−3125.
(24) Tinoco, I., Jr., Sauer, K., and Wang, J. C. (1985) *Physical Chemistry. Principles and Applications in Biological Sciences*, 2nd ed., Prentice-Hall, New Jersey.
(25) Lim, C., Bashford, D., and Karplus, M. (1991) Absolute pK_a calculations with continuum dielectric methods. *J. Phys. Chem.* **95**, 5610−5620.
(26) Topol, I. A., Tawa, G. J., Burt, S. K., and Rashin, A. A. (1997) Calculation of absolute and relative acidities of substituted imidazoles in aqueous solvent. *J. Phys. Chem. A* **101**, 10075−10081.
(27) Jaguar 4.0 (2000) Schrödinger Inc., Portland, OR.
(28) Greeley, B. H., Russo, T. V., Mainz, D. T., Friesner, R. A., Langlois, J.-M., Goddard, W. A., III, Donnelly, R. E., Jr., and Ringalda, M. N. (1994) New pseudospectral algorithms for electronic structure calculations: Length scale separation and analytical 2-electron integral corrections. *J. Chem. Phys.* **101**, 4028−4041.
(29) Slater, J. C. (1974) *Quantum Theory of Molecules and Solids. Vol. 4. The Self-Consistent Field for Molecules and Solids*, McGraw-Hill, New York.
(30) Becke, A. D. (1988) Density-functional exchange-energy approximation with correct asymptotic behavior. *Phys. Rev. A* **38**, 3098−3100.
(31) Vosko, S. H., Wilk, L., and Nusair, M. (1980) Accurate spin-dependent electron liquid correlation energies for local spin density calculations: a critical analysis. *Can. J. Phys.* **58**, 1200−1211.
(32) Lee, C., Yang, W., and Parr, R. G. (1988) Development of the Colle-Salvetti correlation-energy formula into a functional of the electron density. *Phys. Rev. B* **37**, 785−789.
(33) Miehlich, B., Savin, A., Stoll, H., and Preuss, H. (1989) Results obtained with the correlation-energy density functionals of Becke and Lee, Yang, and Parr. *Chem. Phys. Lett.* **157**, 200−206.
(34) Hunter, E. P. L., and Lias, S. G. (1998) Evaluated gas phase basicities and proton affinities of molecules: An update. *J. Phys. Chem. Ref. Data* **27**, 413−656.
(35) Greco, F., Liguori, A., Sindona, G., and Uccella, N. (1990) Gas-phase proton affinity of deoxyribonucleosides and related nucleobases by fast atom bombardment tandem mass spectrometry. *J. Am. Chem. Soc.* **112**, 9092−9096.
(36) Honig, B., Sharp, K., and Yang, A.-S. (1993) Macroscopic models of aqueous solutions: Biological and chemical applications. *J. Phys. Chem.* **97**, 1101−1109.
(37) Tannor, D. J., Marten, B., Murphy, R., Friesner, R. A., Sitkoff, D., Nicholls, A., Ringnalda, M., Goddard, W. A., III, and Honig, B. (1994) Accurate first principles calculation of molecular charge distributions and solvation energies from *ab initio* quantum mechanics and continuum dielectric theory. *J. Am. Chem. Soc.* **116**, 11875−11882.
(38) Honig, B., and Nicholls, A. (1995) Classical electrostatics in biology and chemistry. *Science* **268**, 1144−1149.
(39) Marten, B., Kim, K., Cortis, C., Friesner, R. A., Murphy, R. B., Ringnalda, M. N., Sitkoff, D., and Honig, B. (1996) New model for calculation of solvation free-energies: Correction of self-consistent reaction field continuum dielectric theory for short-range hydrogen-bonding effects. *J. Phys. Chem.* **100**, 11775−11788.
(40) Nicholls, A., and Honig, B. (1991) A rapid finite-difference algorithm, utilizing successive over-relaxation to solve the Poisson−Boltzmann equation. *J. Comput. Chem.* **12**, 435−445.
(41) Archer, D. G., and Wang, P. (1990) The dielectric constant of water and Debye−Hueckel limiting law slopes. *J. Phys. Chem. Ref. Data* **19**, 371−411.
(42) Chirlian, L. E., and Francl, M. M. (1987) Atomic charges derived from electrostatic potentials: a detailed study. *J. Comput. Chem.* **8**, 894−905.
(43) Woods, R. J., Khalil, M., Pell, W., Moffat, S. H., and Smith, V. H., Jr. (1990) Derivation of net atomic charges from molecular electrostatic potentials. *J. Comput. Chem.* **11**, 297−310.
(44) Breneman, C. M., and Wiberg, K. B. (1990) Determining atom-centered monopoles from molecular electrostatic potentials. The need for high sampling density in formamide conformational analysis. *J. Comput. Chem.* **11**, 361−373.
(45) Marcus, Y. (1985) *Ion Solvation*, John Wiley and Sons, Ltd.
(46) Reiss, H., and Heller, A. (1985) The absolute potential of the standard hydrogen electrode: A new estimate. *J. Phys. Chem.* **89**, 4207−4213.
(47) Tissandier, M. D., Cowen, K. A., Feng, W. Y., Gundlach, E., Cohen, M. H., Earhart, A. D., Coe, J. V., and Tuttle, T. R., Jr. (1998) The proton's absolute aqueous enthalpy and Gibbs free energy of solvation from cluster-ion solvation data. *J. Phys. Chem. A* **102**, 7787−7794.
(48) Shigenaga, M. K., Gimeno, C. J., and Ames, B. N. (1989) Urinary 8-hydroxy-2′-deoxyguanosine as a biological marker of in vivo oxidative DNA damage. *Proc. Natl. Acad. Sci. U.S.A.* **86**, 9697−9701.
(49) Kasai, H., Crain, P. F., Kuchino, Y., Nishimura, S., Ootsuyama, A., and Tanooka, H. (1986) Formation of 8-hydroxyguanine moiety in cellular DNA by agents producing oxygen radicals and evidence for its repair. *Carcinogenesis* **7**, 1849−1851.
(50) Floyd, R. A., Watson, J. J., Harris, J., West, M., and Wong, P. K. (1986) Formation of 8-hydroxydeoxyguanosine, hydroxyl free-radical adduct of DNA in granulocytes exposed to the tumor promoter, tetradeconylphorbolacetate. *Biochem. Biophys. Res. Commun.* **137**, 841−846.
(51) Kasai, H. (1997) Analysis of a form of oxidative DNA damage, 8-hydroxy-2′-deoxyguanosine, as a marker of cellular oxidative stress during carcinogenesis. *Mutat. Res.* **387**, 147−163.
(52) Kawanishi, S., Hiraku, Y., and Oikawa, S. (2001) Mechanism of guanine-specific DNA damage by oxidative stress and its role in carcinogenesis and aging. *Mutat. Res.* **488**, 65−76.
(53) Echols, H., and Goodman, M. F., (1991) Fidelity mechanisms in DNA replication. *Annu. Rev. Biochem.* **60**, 477−511.
(54) Dinner, A. R., Blackburn, G. M., and Karplus, M. (2001) Uracil-DNA glycosylase acts by substrate autocatalysis. *Nature* **413**, 752−755.
(55) Werner, R. M., and Stivers, J. T. (2000) Kinetic isotope effect studies of the reaction catalyzed by uracil DNA glycosylase: evidence for an oxocarbenium-ion uracil anion intermediate. *Biochemistry* **39**, 14054−14064.
(56) Zharkov, D. O., Rosenquist, T. A., Gerchman, S. E., and Grollman, A. P. (2000) Substrate specificity and reaction mechanism of murine 8-oxoguanine-DNA glycosylase. *J. Biol. Chem.* **275**, 28607−28617.
(57) Nash, H. M., Lu, R., Lane, W. S., and Verdine, G. L. (1997) The critical active-site amine of the human 8-oxoguanine DNA glycosylase, hOgg1: Direct identification, ablation and chemical reconstitution. *Chem. Biol.* **4**, 693−702.
(58) Lide, D. R. (1999−2000) *CRC Handbook of Chemistry and Physics*, 80th ed., CRC Press, Boca Raton.
(59) Dawson, R. M. C., Elliott, D. C., Elliott, W. H., and Jones, K. M. (1986) *Data for Biochemical Research*, 3rd ed., Oxford University Press, Oxford.
(60) Fasman, G. D. (1975) *CRC Handbook of Biochemistry and Molecular Biology. Nucleic Acids*, Vol. 1, 3rd ed., CRC Press, Cleveland, OH.
(61) Ts'o, P. O. P. (1974) *Basic Principles in Nucleic Acid Chemistry*, Academic Press, New York.
(62) Jordan, D. O. (1960) *The Chemistry of Nucleic Acids*, Butterworth and Co., Washington.
(63) Chargaff, E., and Davidson, J. N. (1955) *The Nucleic Acids. Chemistry and Biology*, Academic Press Inc., New York.
(64) Bundari, S. (1996) *The Merck Index*, 12th ed., Merck and Co., Inc., Whitehouse Station, NJ.

TX010146R